Electronic Supplementary Material (ESI) for Journal of Materials Chemistry A.

CdS-Phenanthroline Derivative Hybrid Cathode Interlayers for High Performance Inverted Organic Solar Cells

Xiaohui Liu,[†,a,b] Yulei Wu,[†,a] Xiaodong Li,[a,b] Wenjun Zhang,[a] Lixiao Zhao,[a] Hai-Qiao Wang*,[a] and Junfeng Fang*,[a]

[a] Ningbo Institute of Materials Technology and Engineering, Chinese Academy of Sciences, Ningbo 315201, China

[b] University of Chinese Academy of Sciences, Beijing 100049, China

[†] Xiaohui Liu and Yulei Wu contributed equally to this work.

Email: hqwang@nimte.ac.cn, fangjf@nimte.ac.cn

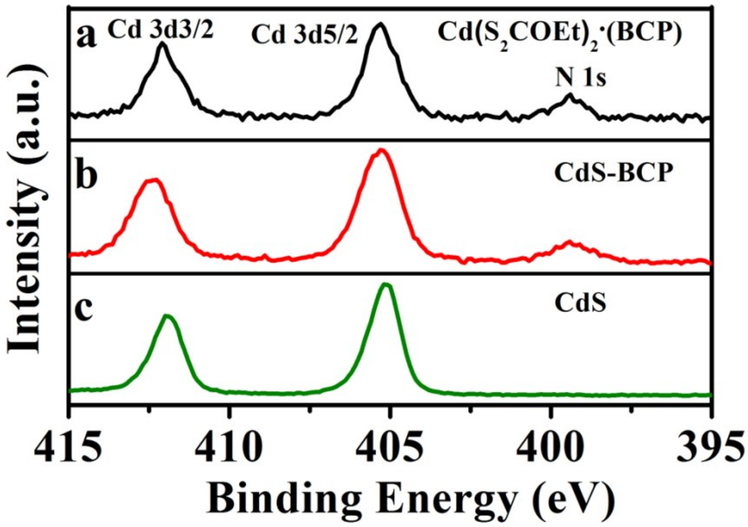

Fig. S1 XPS spectra of (a) Cd3d peak and N1s peak of the precursor $Cd(S_2COEt)_2$·(BCP), (b) Cd3d peak and N1s peak of the CdS-BCP decomposed from $Cd(S_2COEt)_2$·(BCP), (c) Cd3d peak of CdS decomposed from $Cd(S_2COEt)_2$·$(Pyridine)_2$.

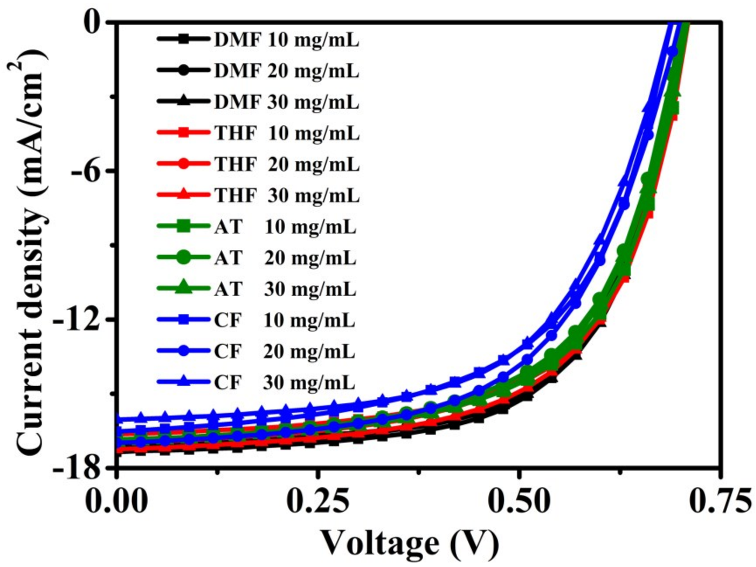

Fig. S2 Current-voltage characteristics of OSCs incorporating CdS-BCP as cathode interlayer under AM 1.5G irradiation. The CdS-BCP films were spin-cast from various solvents with different concentration. Device configuration: ITO/CdS-BCP/PTB7:$PC_{71}BM$/MoO_3/Al.

Table S1. Performance of devices fabricated on CdS-BCP cathode interlayer deposited from various solvents and different concentration, AM 1.5G irradiation ($100\ mW\cdot cm^{-2}$).

Solvent & concentration	V_{oc} V	Jsc $mA\cdot cm^{-2}$	FF %	PCE (%) Best	PCE (%) Avg	R_s $\Omega\cdot cm^2$	R_{sh} $K\Omega\cdot cm^2$
DMF 10 mg/mL (15±3 nm)	0.706	17.35	63.32	7.76	7.52	5.67	0.66
DMF 20 mg/mL (26±2 nm)	0.707	17.01	63.94	7.69	7.57	5.61	1.09
DMF 30 mg/mL (33±3 nm)	0.707	17.21	63.81	7.76	7.42	5.19	0.85
THF 10 mg/mL (16±3 nm)	0.709	16.61	63.73	7.51	7.28	5.16	0.90
THF 20 mg/mL (29±4 nm)	0.710	16.94	61.07	7.34	7.17	6.45	0.86
THF 30 mg/mL (38±4 nm)	0.706	17.20	62.72	7.62	7.37	5.16	0.81
AT 10 mg/mL (18±5 nm)	0.709	16.81	62.58	7.46	7.25	5.45	0.84
AT 20 mg/mL (30±6 nm)	0.701	16.85	61.51	7.26	7.11	5.05	0.70
AT 30 mg/mL (39±5 nm)	0.705	16.89	61.86	7.37	7.27	5.66	0.77
CF 10 mg/mL (20±4 nm)	0.689	16.52	58.30	6.64	6.53	7.06	0.57
CF 20 mg/mL (33±5 nm)	0.699	16.95	58.63	6.95	6.75	7.79	0.76
CF 30 mg/mL (44±4 nm)	0.688	16.03	59.95	6.61	6.45	8.14	0.84

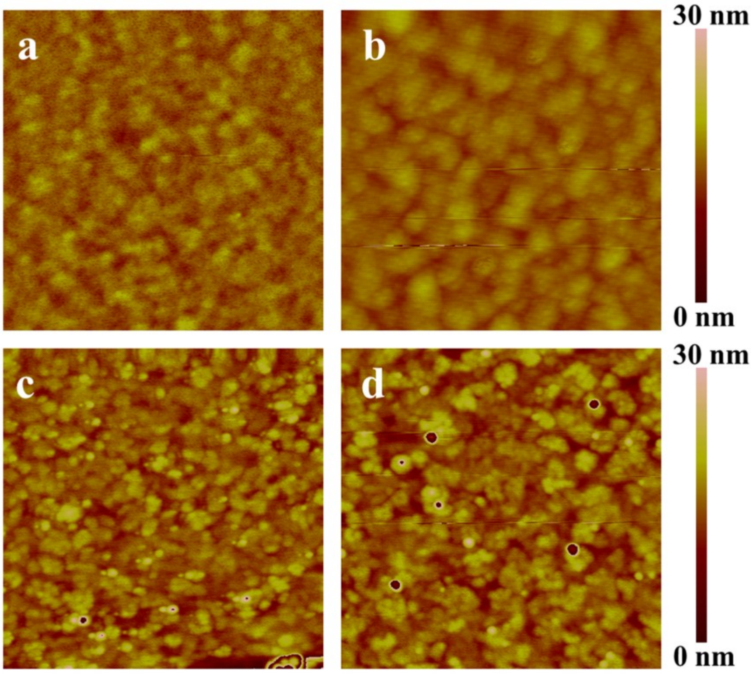

Fig. S3 AFM height images (10.0μm×10.0μm) of hybrid CdS-BCP interlayers with different solvents (a) DMF, (b) THF, (c) AT and (d) CF, respectively. The height bar is 50 nm.

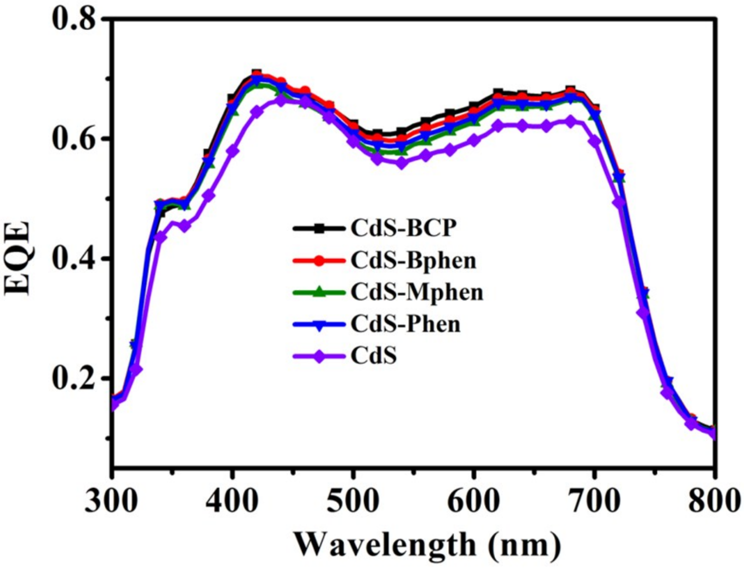

Fig. S4 EQE of devices incorporating CdS-P and CdS as cathode interlayers measured in air with a larger spot size than the device area.

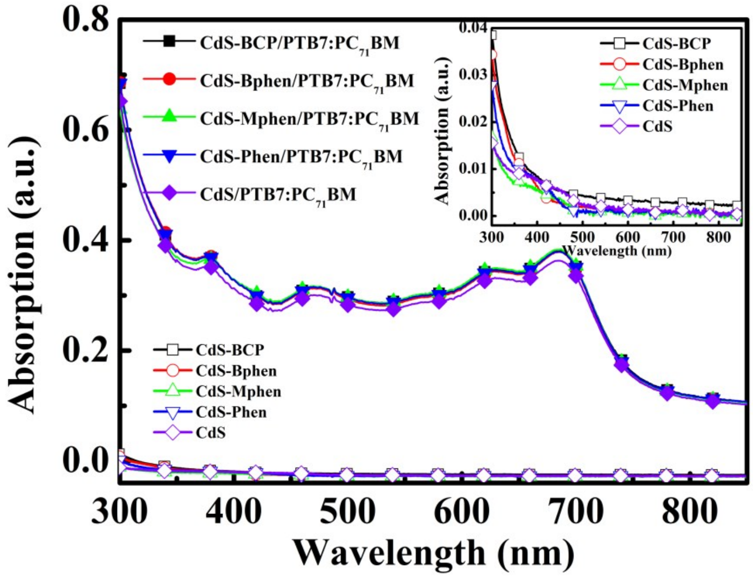

Fig. S5 Absorption spectra of hybrid CdS-P (BCP, Bphen, Mphen and Phen) interlayers and the CdS-P/PTB7:$PC_{71}BM$ films on quartz substrate. The inset figure shows the zoom in view of the absorption spectra of hybrid CdS-P films.

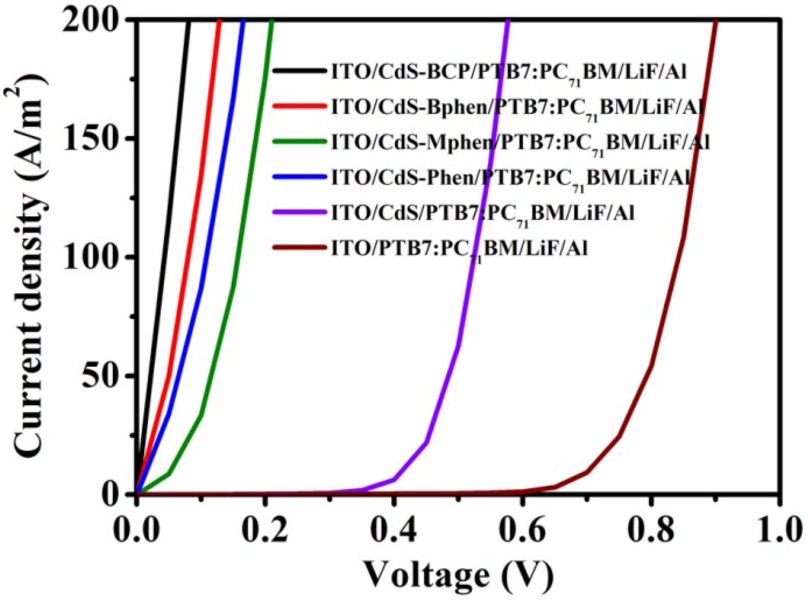

Fig. S6 J-V curves of electron-only devices. CdS or CdS-P is used as electron-transporting layers, and device with bare ITO (without any electron transport layers) was fabricated for comparison.

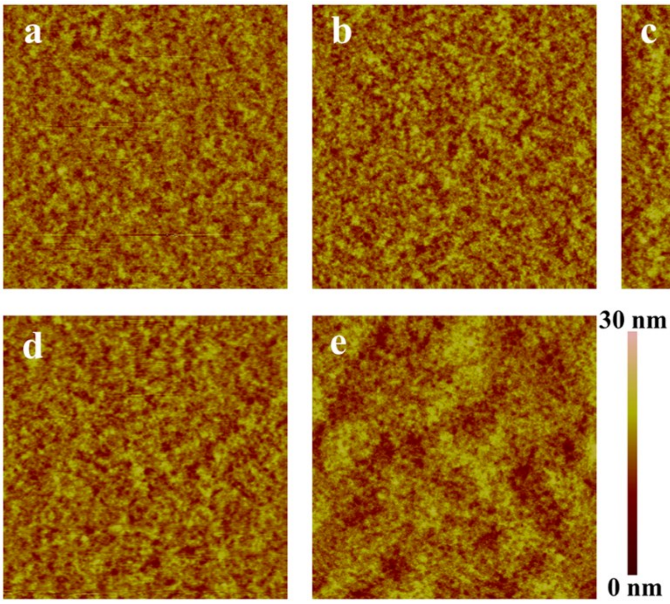

Fig. S7 AFM height images (2.0μm×2.0μm) of PTB7:$PC_{71}BM$ films on different hybrid cathode interlayer. (a) CdS-BCP, (b) CdS-Bphen, (c) CdS-Mphen, (d) CdS-Phen and (e) CdS, respectively. The height bar is 30 nm.

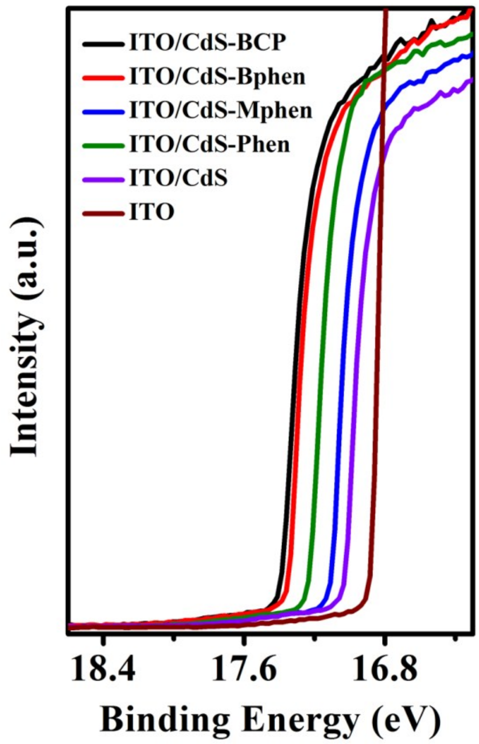

Fig. S8 UPS measurement of CdS, and CdS-P films on ITO. Films of CdS and CdS-P were decomposed from its precursors on ITO after annealing at 175 °C for 30 min.